

Enhanced Activity of Monomethylauristatin F through Monoclonal Antibody Delivery: Effects of Linker Technology on Efficacy and Toxicity

Svetlana O. Doronina,* Brian A. Mendelsohn, Tim D. Bovee, Charles G. Cervený, Stephen C. Alley, Damon L. Meyer, Ezogelin Oflazoglu, Brian E. Toki, Russell J. Sanderson, Roger F. Zabinski, Alan F. Wahl, and Peter D. Senter

Seattle Genetics, Inc., 21823 30th Drive SE, Bothell, Washington 98021. Received October 4, 2005; Revised Manuscript Received October 19, 2005

We have previously shown that antibody–drug conjugates (ADCs) consisting of cAC10 (anti-CD30) linked to the antimetabolic agent monomethylauristatin E (MMAE) lead to potent in vitro and in vivo activities against antigen positive tumor models. MMAF is a new antimetabolic auristatin derivative with a charged C-terminal phenylalanine residue that attenuates its cytotoxic activity compared to its uncharged counterpart, MMAE, most likely due to impaired intracellular access. In vitro cytotoxicity studies indicated that mAb–maleimidocaproyl–valine–citrulline–*p*-aminobenzyloxycarbonyl–MMAF (mAb–L1–MMAF) conjugates were >2200-fold more potent than free MMAF on a large panel of CD30 positive hematologic cell lines. As with cAC10–L1–MMAE, the corresponding MMAF ADC induced cures and regressions of established xenograft tumors at well tolerated doses. To further optimize the ADC, several new linkers were generated in which various components within the L1 linker were either altered or deleted. One of the most promising linkers contained a noncleavable maleimidocaproyl (L4) spacer between the drug and the mAb. cAC10–L4–MMAF was approximately as potent in vitro as cAC10–L1–MMAF against a large panel of cell lines and was equally potent in vivo. Importantly, cAC10–L4–MMAF was tolerated at >3 times the MTD of cAC10–L1–MMAF. LCMS studies indicated that drug released from cAC10–L4–MMAF was the cysteine–L4–MMAF adduct, which likely arises from mAb degradation within the lysosomes of target cells. This new linker technology appears to be ideally suited for drugs that are both relatively cell-impermeable and tolerant of substitution with amino acids. Thus, alterations of the linker have pronounced impacts on toxicity and lead to new ADCs with greatly improved therapeutic indices.

INTRODUCTION

In recent years, the impact that monoclonal antibodies (mAbs)¹ have had in the clinical treatment of cancer has been pronounced. There are now several approved therapeutic antibodies, including trastuzumab (Herceptin), rituximab (Rituxan), cetuximab (Erbix), and bevacizumab (Avastin), and many others are in late-stage development (reviewed in refs 1, 2). While these agents display significant activities through such mechanisms as antibody-dependent cellular cytotoxicity, complement-dependent cytotoxicity, and signal transduction, the activities are generally suboptimal, even when combined with conventional cancer chemotherapeutic agents. Consequently, significant attention has turned toward the use of mAb-based immunoconjugates, in which the mAb carries a toxic payload

to tumor cells (reviewed in refs 3, 4). Three such agents are now clinically approved: ibritumomab tiuxetan (Zevalin), a ⁹⁰Y labeled anti-CD20 mAb; tositumomab (Bexxar), an ¹³¹I labeled anti-CD20 mAb; and gemtuzumab ozogamicin (Mylotarg), an anti-CD33–calicheamicin conjugate. The activities of these conjugated mAbs provide validation for the concept, and a basis for developing other such agents for cancer therapy.

The goal of targeted therapy with mAb–drug conjugates is to achieve high degrees of therapeutic activity, while sparing normal tissues from chemotherapeutic damage. Toward this end, several critical parameters have been identified that must be addressed. These include the barriers to mAb extravasation, conjugate immunogenicity, widespread expression of the target antigen on normal tissue, metabolism at nontarget sites, low drug potency, and efficient release of the drug in forms that do not impair activity (3–6). Consequently, the focus in many laboratories has been to use chimeric or humanized mAbs against highly selective tumor-associated antigens, attached to potent drugs through linkers that allow for efficient drug release once the antibody–drug conjugate (ADC) has bound to the target and has undergone internalization. Examples of some advanced agents include C242-DM1 (cintuzumab mertansine), an anticarcinoma mAb linked to a derivative of maytansine (7), MLN2704, an anti-prostate cancer mAb attached to maytansine (5), and an anti-CD22–calicheamicin conjugate for the treatment of B-cell lymphomas (8).

In developing highly active agents that address the issues described for targeted therapy, we have focused considerable attention on the drug payload, the linker used for drug attachment, and the method by which the antibody is modified. This has led to the development of mAb–auristatin conjugates

* To whom correspondence should be addressed. E-mail: sdoronina@seagen.com

¹ Abbreviations: ADC, antibody–drug conjugate; cAC10–linker–drug₄ or ₈, cAC10 ADC with four or eight drugs/mAb; Cit, L-citrulline; Cys, L-cysteine; Dap, dolaproine; DEPC, diethyl cyanophosphonate; DIEA, *N,N*-diisopropylethylamine; Dil, dolaisoleuine; DMF, dimethylformamide; DTNB, 5,5′-dithio-bis(2-nitrobenzoic acid); DTT, dithiothreitol; Fmoc, 9-fluorenylmethoxycarbonyl; HATU, *O*-(7-azabenzotriazol-1-yl)-*N,N,N'*,*N'*-tetramethyluronium hexafluorophosphate; HRP, horseradish peroxidase; IC₅₀, dose that inhibits cell growth by 50%; L1–4, linkers 1–4 (Table 1); MeVal, *N*-methyl valine; mAb, monoclonal antibody; MDR, multidrug resistance; MMAE, monomethylauristatin E; MMAF, monomethylauristatin F; MMAF-OME, monomethylauristatin F methyl ester; MTD, maximum tolerated dose; PAB, *p*-aminobenzylyl; PABC, *p*-aminobenzyloxycarbonyl; PABOH, *p*-aminobenzylyl alcohol; PBS, phosphate-buffered saline; Phe, L-phenylalanine; pNP, *p*-nitrophenyl; TFA, trifluoroacetic acid; Val, L-valine.

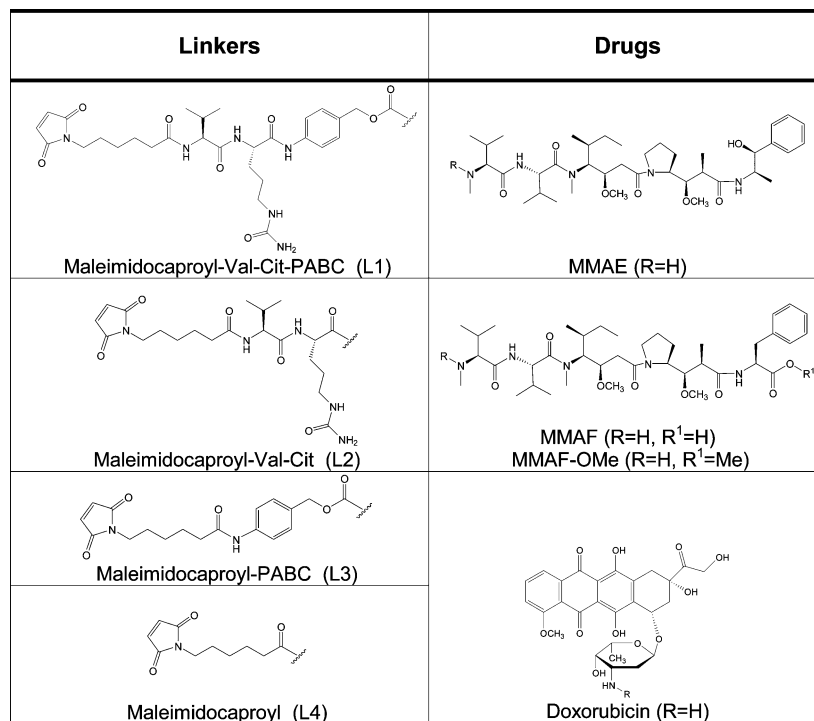


Figure 1. Structures of drugs and linkers.

that include a highly potent and totally synthetic drug attached to mAb cysteine residues through a proteolytically cleavable linker (3, 6, 9–12). The most advanced agent that we have described (12–15) is cAC10–maleimidocaproyl-valine-citrulline-*p*-aminobenzyloxycarbonyl-monomethylauristatin E (cAC10–maleimidocaproyl-Val-Cit-PABC–MMAE, or cAC10–L1–MMAE, shown in Figure 1). This is comprised of the highly potent antimetabolic agent MMAE, attached to mAb–cysteines through the L1 linker that is cleaved by intracellular proteases such as cathepsin B. The optimal number of drugs/mAb was found to be four (14), where pronounced activities at well tolerated doses were obtained in CD30 positive hematologic malignancies.

Here, we describe the properties of a new auristatin, MMAF, that was designed to be much more active when actively delivered inside cells with a mAb, compared to treatment in the untargeted form. We viewed such an approach to targeted delivery as advantageous compared to that of drugs that have high potency in the untargeted form, since any drug that is systemically released would not be expected to contribute to toxic side-effects. Several linker technologies were evaluated to optimize the delivery of MMAF to target cells. In this report, we demonstrate that targeted MMAF is much more potent than the free drug, and that cAC10 conjugates of MMAF display pronounced activities, both in vitro and in vivo. In addition, conjugates of MMAF circumvent a common form of multidrug resistance (MDR). The development of this drug, together with the biological activities of ADCs derived from it, are described for the first time.

EXPERIMENTAL PROCEDURES

General. Unless otherwise noted, materials were obtained from commercial suppliers in the highest purity grade available and used without further purifications. Anhydrous DMF and CH₂Cl₂ were purchased from Aldrich. *N*-Fmoc-L-[ring-¹³C₆]-Phenylalanine was obtained from Cambridge Isotope Laboratories, Inc. (Andover, MA). 2-Chlorotrityl chloride resin was purchased from Advanced ChemTech and loaded with *N*-Fmoc-

L-[ring-¹³C₆]-phenylalanine according to manufacturer's specifications. Phenylalanine-2-chlorotrityl resin was purchased from Novabiochem. Phenylalanine loading level of the resin was determined (0.55 mmol/gram) by extensive acylation with Fmoc-Cl followed by spectrophotometric Fmoc-quantitation assay. Solid-phase synthesis was performed in plastic syringes (National Scientific Company) fitted with a filter cut out of fritware PE medium grade porous sheet (Scienceware). Burrell wrist action shaker (Burrell Scientific, Pittsburgh, PA) was used for agitation. All solid-phase yields reported are based upon the initial phenylalanine substitution level of the resin and constitute a mass balance of isolated pure material from support, unless otherwise stated. Fmoc-Dap was custom synthesized by Albany Molecular Research, Inc. (Albany, NY).

HPLC assays were performed using C12 Phenomenex Synergy MAX-RP 4 μ , 80 Å reversed-phase column, 150 × 2.0 mm. The eluent was a linear gradient of acetonitrile from 5% to 95% in 5 mM aqueous ammonium phosphate, pH 7.0, in 10 min, then 95% acetonitrile for 10 min, flow rate 1 mL/min, 215 nm detection. Preparative HPLC purifications were performed on Varian instrument equipped with C12 Phenomenex Synergy MAX-RP 4 μ reversed phase column, 250 × 21.2 mm, eluting with 0.1% TFA in a water–acetonitrile gradient. Flash chromatography was carried out using Whatman 60 Å 230–400 mesh ASTM silica gel.

Low resolution mass spectra (LCMS) were recorded on a ZMD-Micromass Single Quadrupole Mass Spectrometer equipped with an electrospray ion source (45 eV) coupled with HP1100 HPLC system (reverse phase C12 Phenomenex column, 4 μ , 100 Å, 150 × 2.0 mm). The eluent was a linear gradient of acetonitrile from 5% to 95% in water in the presence of 0.1% formic acid in 10 min, then 95% acetonitrile for 5 min, flow rate 400 μ L/min). High resolution (exact mass, HRMS) electrospray ionization (ESI) data were obtained at the University of Washington Medicinal Chemistry Mass Spectrometry Center on a Bruker APEXIII 47e [FT(ICR)]MS. NMR data were recorded on Varian Mercury 400 MHz Instrument. Chemical shifts (δ) are reported in ppm downfield from an internal solvent peak, and *J* values are in hertz.

The chimeric IgG₁ cAC10 (16) and cBR96 (17) mAbs recognize the CD30 and Lewis Y antigens, respectively. The human lymphoma cell lines Karpas 299, SUP-M2, SU-DHL-1, SR-786, DEL, HDLM-2, L428, KMH-2, and WSU-NHL were obtained from the DSMZ (Braunschweig, Germany). 786-O and Caki-1 renal cell carcinoma and HH lymphoma cell lines were purchased from the ATCC (Manassas, VA). H3396 breast carcinoma cells were obtained as described earlier (16). The parent/drug resistant cell line pair NCI-H69, NCI-H69/LX4 were obtained from the ECACC (Salisbury, England), and the Hodgkin's disease cell line L540cy has been previously described (18). All cell lines were grown according to the manufacturers' recommendations and routinely checked for mycoplasma contamination.

Maleimidocaproyl-MMAE (L4-MMAE). To a solution of MMAE (12) (72 mg, 0.1 mmol) in anhydrous CH₂Cl₂ (2 mL) 6-maleimidocaproic acid (30 mg, 0.15 mmol, 1.5 equiv) was added followed by DEPC (36 μ L, 0.2 mmol, 2 equiv) and DIEA (55 μ L, 0.3 mmol, 3 equiv). The reaction mixture was stirred at room temperature for 2 h. CH₂Cl₂ (30 mL) was added, and the mixture was washed with 10% aqueous citric acid (2 \times 20 mL), water (20 mL), and brine (20 mL) and concentrated to near dryness. Product was isolated by flash chromatography on silica gel eluting with 5% MeOH in CH₂Cl₂ to give a white solid, 32 mg (35%). Reversed-phase HPLC analysis: 98% at 9.48 min. ¹H NMR (DMSO-*d*₆): δ 0.70–0.89 (18H, m), 0.95–1.05 (6H, m), 1.19–1.34 (m), 1.44–1.55 (m), 1.66–1.84 (m), 1.88–2.02 (m), 2.06–2.16 (m), 2.22–2.46 (m), 2.81 (s), 2.86 (s), 2.90 (s), 2.93 (s), 2.97 (d), 3.01–3.08 (m), 3.12 (d), 3.17 (d), 3.20 (d), 3.23 (dd), 3.35–3.40 (m), 3.42–3.50 (m), 3.52–3.59 (m), 3.77 (d), 3.93–4.04 (m), 4.37–4.54 (m), 4.59–4.64 (m), 4.70–4.78 (m), 5.36 (d), 5.43 (d), 7.01–7.02 (2H, m), 7.14–7.31 (5H, m), 7.65 (d), 7.74 (d), 7.78 (d), 7.89–7.92 (m), 8.56–8.61 (m). HRMS (ESI) calcd for C₄₉H₇₉N₆O₁₀ (MH)⁺ 911.5858; found, *m/z* 911.5839.

Fmoc-MMAF-OMe. Fmoc-MeVal-Val-Dil (12) (0.50 g, 0.78 mmol) and Dap-Phe-OMe·HCl (12) (0.30 g, 0.78 mmol) were dissolved in CH₂Cl₂ (5 mL) followed by the addition of DIEA (0.30 mL, 1.71 mmol, 2.2 equiv). DEPC (0.20 mL, 1.17 mmol, 1.5 equiv) was added next while the contents stirred under Ar. Reaction was complete according to HPLC analysis after 1 h. The mixture was concentrated and purified on silica gel eluting with a step gradient of ethyl acetate (from 50% to 100%) in hexane to provide a white foam, 0.65 g (87%). Reversed-phase HPLC analysis: 95% at 16.2 min. ¹H NMR (DMSO-*d*₆): δ 0.71–0.95 (20H, m), 1.01–1.07 (3H, dd), 1.22–1.30 (m), 1.34–1.52 (m), 1.60–1.83 (m), 1.92–2.11 (m), 2.16–2.28 (2H, m), 2.31–2.42 (m), 2.79–2.89 (m), 2.96–3.07 (m), 3.15–3.16 (m), 3.19 (s), 3.24 (s), 3.29 (d), 3.42–3.55 (m), 3.63 (1.5H, s), 3.66 (1.5H, s), 3.75 (0.5H, d), 3.96 (1H, m), 4.09–4.11 (m), 4.21–4.51 (m), 4.61–4.74 (m), 7.15–7.23 (5H, m), 7.31 (2H, t), 7.41 (3H, t), 7.62 (2H, d), 7.89 (2H, d), 8.05 (0.5H, d), 8.11 (0.5H, d), 8.29 (0.5H, d), 8.51 (0.5H, d). LCMS (ESI): *m/z* 968.35 (MH)⁺ (eluted at 14.84 min).

MMAF-OMe. Fmoc-MMAF-OMe (140 mg, 0.14 mmol) in CH₂Cl₂ (5 mL) was treated with diethylamine (2 mL). After 2 h, the reaction was concentrated and purified by preparative HPLC to give a TFA salt of MMAF-OMe as a white solid, 126 mg (98%). Reversed-phase HPLC analysis: 94% at 11.25 min. ¹H NMR (DMSO-*d*₆): δ 0.77 (3H, m), 0.87–1.07 (19H, m), 1.22–1.32 (m), 1.37–1.52 (m), 1.60–1.88 (m), 1.96–2.12 (m), 2.18–2.29 (m), 2.32–2.54 (m), 2.83–2.90 (m), 2.99 (s), 3.07 (s), 3.16–3.20 (m), 3.26 (s), 3.42–3.58 (m), 3.64 (s), 3.66 (s), 3.75 (d), 3.98 (m), 4.43–4.52 (m), 4.55–4.76 (m), 7.17–7.58 (5H, m), 8.30 (0.5H, d), 8.56 (0.5H, d), 8.83–8.93 (3H, m). HRMS (ESI) calcd for C₄₀H₆₈N₅O₈ (MH)⁺ 746.5068; found, *m/z* 746.5037.

Maleimidocaproyl-Val-Cit-PABC-MMAF-OMe (L1-MMAF-OMe). MMAF-OMe·TFA (110 mg, 0.13 mmol, 1.0 equiv), maleimidocaproyl-Val-Cit-PAB-OCO-pNP (10) (103 mg, 0.14 mmol, 1.1 equiv), and 1-hydroxybenzotriazole (HOBt, 3.4 mg, 26 μ mol, 0.2 equiv) were dissolved in pyridine (0.5 mL) and DMF (2 mL) under Ar. To this mixture was added DIEA (22.5 μ L, 0.13 mmol, 1.0 equiv). The resulting solution stirred for 3 h before more DIEA (22.5 μ L) was added. After stirring for 40 h total, the mixture was concentrated, taken up in DMSO (2 mL). Preparative HPLC purification followed by precipitation from CH₂Cl₂ (2 mL) with ether resulted in 90 mg (52%) of white solid. Reversed-phase HPLC analysis: 95% at 9.48 min. ¹H NMR (DMSO-*d*₆): δ 0.72–0.94 (28H, m), 1.02–1.06 (3H, dd), 1.14–1.52 (m), 1.54–1.82 (m), 1.90–2.38 (m), 2.28–2.46 (m), 2.85 (br s), 2.97 (s), 3.04 (s), 3.16 (s), 3.18 (s), 3.20 (s), 3.25 (s), 3.28–3.30 (m), 3.42–3.58 (m), 3.63 (s), 3.66 (s), 3.75 (d), 3.96 (m), 4.17–4.21 (m), 4.23–4.28 (m), 4.32–4.42 (m), 4.44–4.55 (m), 4.60–4.74 (m), 4.94–5.12 (m), 6.01 (1H, br s), 7.01 (2H, s), 7.18–7.32 (9H, m), 7.58 (2H, m), 7.81 (1H, d), 8.07–8.12 (1.5H, m), 8.29 (1H, m), 8.51 (0.5H, d), 10.0 (1H, d). HRMS (ESI) calcd for C₆₉H₁₀₆N₁₁O₁₆ (MH)⁺ 1344.7819; found, *m/z* 1344.7776.

Maleimidocaproyl-PAB-OCO-pNP. To a suspension of 6-maleimidocaproic acid (1.0 g, 4.52 mmol) in CH₂Cl₂ (13.0 mL) was added *p*-aminobenzyl alcohol (PABOH, 1.11 g, 9.04 mmol, 2.0 equiv) and 2-ethoxy-1-ethoxycarbonyl-1,2-dihydroquinoline (EEDQ, 2.24 g, 9.04 mmol, 2.0 equiv). The reaction mixture was stirred at ambient temperature for 16 h, and then concentrated to near dryness. The residue was purified by flash chromatography on silica gel, eluting with a step gradient from 25 to 100% ethyl acetate in hexane, to give 1.38 g (96%) of maleimidocaproyl-PABOH as a white solid. Maleimidocaproyl-PABOH (0.85 g, 2.69 mmol) was then activated by reaction with bis *p*-nitrophenyl carbonate (2.45 g, 8.07 mmol, 3 equiv) and DIEA (0.94 mL, 5.38 mmol, 2 equiv) in DMF (10 mL). After 1 h, HPLC analysis indicated complete consumption of starting material. Solvent was removed under reduced pressure, and the residue was triturated with diethyl ether (5 \times 20 mL) resulting in 1.25 g (96%) of an off white solid. Reversed-phase HPLC analysis: 99% at 9.98 min. ¹H NMR (CDCl₃): δ 1.37 (2H, m), 1.64 (2H, m), 1.77 (2H, m), 2.37 (2H, t, *J* = 7.6), 3.54 (2H, t, *J* = 7.2), 6.68 (2H, s), 7.37 (2H, d, *J* = 9.2), 7.41 (2H, d, *J* = 8.8), 7.57 (2H, d, *J* = 8.8), 8.27 (2H, d, *J* = 9.2).

MeVal-Val-Dil-Dap-Phe-2-chlorotrityl Resin. Fmoc-Dap (450 mg, 1.1 mmol) and HATU (418 mg, 1.1 mmol, 2 equiv) were dissolved in anhydrous DMF (8 mL), and DIEA (384 μ L, 2.2 mmol, 4 equiv). The resulting solution was added to the 20 mL syringe containing Phe-2-chlorotrityl resin (1 g, 0.55 mmol). Mixture was agitated for 3 h. Reaction completion was determined by LCMS analysis of material cleaved off a small amount of resin. The resin was filtered, washed with DMF (6 \times 10 mL), CH₂Cl₂ (6 \times 10 mL), ethyl ether (6 \times 10 mL), and dried in vacuo for 2 h. A 20% piperidine in DMF solution (5 mL) was added to the syringe, and the mixture was agitated for 2 h. The resin was then filtered, rinsed with DMF (6 \times 10 mL), CH₂Cl₂ (6 \times 10 mL), and ethyl ether (6 \times 10 mL), and dried in vacuo. In a separate flask Fmoc-MeVal-Val-Dil tripeptide (12) (702 mg, 1.1 mmol) and HATU (418 mg, 1.1 mmol, 2 equiv) were dissolved in anhydrous DMF (8 mL) followed by the addition of DIEA (384 μ L, 2.2 mmol, 4 equiv). The solution was then transferred to the syringe containing the resin, and the mixture was agitated for 3 h. LCMS analysis of material cleaved from a small amount of resin was used to determine reaction completion. The resin was filtered, washed with DMF (6 \times 10 mL), CH₂Cl₂ (6 \times 10 mL), and ethyl ether (6 \times 10 mL), and dried in vacuo for 2 h. A 20% piperidine solution in DMF (5 mL) was added to the resin, and the mixture

was agitated for 2 h. The resin was then filtered, washed with DMF (6 × 10 mL), CH₂Cl₂ (6 × 10 mL), and ethyl ether (6 × 10 mL), and dried in vacuo.

MMAF (MeVal-Val-Dil-Dap-Phe). MeVal-Val-Dil-Dap-Phe-2-chlorotrityl resin (100 mg, 0.044 mmol) in a 5 mL syringe was treated with 2% TFA in CH₂Cl₂ (4 mL) for 5 min at ambient temperature. Preparative HPLC purification provided 27 mg (73%) of white solid. Reversed-phase HPLC analysis: 95% at 5.74 min. ¹H NMR (DMF-*d*₇): δ 0.78 (3H, t), 0.90–1.15 (19H, m), 1.28–1.44 (m), 1.46–1.62 (m), 1.75–2.00 (m), 2.03–2.12 (m), 2.14–2.23 (m), 2.24–2.48 (m), 2.50–2.61 (m), 2.78–2.82 (m), 2.97–3.09 (m), 3.12 (s), 3.18–3.21 (m), 3.26 (d), 3.30 (s), 3.34 (s), 3.41–3.46 (m), 3.49 (d), 3.53–3.60 (m), 3.61–3.69 (m), 3.72–3.78 (m), 3.93 (d), 4.10 (2H, br d), 4.12–4.38 (1H, br), 4.64–4.92 (3H, m), 7.21–7.35 (5H, m), 8.12 (0.5H, d), 8.40 (0.5H, d), 8.78–8.83 (1H, m), 9.03 (1H, br s), 9.63 (1H, br s). HRMS (ESI) calcd for C₃₉H₆₆N₅O₈ (MH)⁺ 732.4911; found, *m/z* 732.4890.

Maleimidocaproyl-Val-Cit-PABC–MMAF (L1–MMAF). MeVal-Val-Dil-Dap-Phe-2-chlorotrityl resin (120 mg, 0.053 mmol) in a 5 mL syringe was treated with a solution of maleimidocaproyl-Val-Cit-PAB-OCOPNP (313 mg, 0.42 mmol, 8 equiv), 1-hydroxy-7-azabenzotriazole (HOAt, 2 mg, 0.015 mmol, 0.3 equiv), and DIEA (148 μL, 0.84 mmol, 16 equiv) in DMF (4 mL) for 16 h. The resin was then filtered and washed with DMF (6 × 3 mL), CH₂Cl₂ (6 × 3 mL) and ethyl ether (6 × 3 mL). Cleavage from resin by treatment with 2% TFA in CH₂Cl₂ (4 mL) for 5 min and preparative HPLC purification of the released material generated 15 mg (21%) of white solid that was 98% pure by reversed-phase HPLC analysis (retention time 7.20 min). ¹H NMR (DMSO-*d*₆): δ 0.75–0.95 (28H, m), 1.05 (3H, t), 1.14 (m), 1.22–1.53 (m), 1.53–1.80 (m), 1.80–2.40 (m), 2.80 (br s), 2.96 (d), 3.11 (s), 3.13 (s), 3.20 (s), 3.62–3.70 (d), 3.83–3.94 (m), 4.08–4.24 (m), 4.28–4.5 (m), 4.50–4.68 (m), 4.90–5.10 (m), 5.35 (s), 5.96 (1H, t), 7.02 (2H, s), 7.08–7.32 (9H, m), 7.54 (2H, d), 7.80 (d), 8.04–8.12 (m), 8.16–8.33 (m), 10.0 (1H, br s). HRMS (ESI) calcd for C₆₈H₁₀₄N₁₁O₁₆ (MH)⁺ 1330.7663; found, *m/z* 1330.7665.

Maleimidocaproyl-Val-Cit–MMAF (L2–MMAF). Fmoc-Cit (140 mg, 0.352 mmol) and Fmoc-Val (60 mg, 0.176 mmol) were coupled sequentially to MeVal-Val-Dil-Dap-Phe-2-chlorotrityl resin (200 mg, 0.088 mmol) using HATU coupling chemistry as described above for MeVal-Val-Dil-Dap-Phe-2-chlorotrityl resin. Then, to the dry Val-Cit-MeVal-Val-Dil-Dap-Phe-2-chlorotrityl resin a solution of 6-maleimidocaproic acid *N*-hydroxysuccinimide ester (54 mg, 0.176 mmol) in DMF (3 mL) was added. The mixture was shaken at room temperature for 4 h. Cleavage from resin by treatment with 2% TFA in CH₂Cl₂ (4 mL) for 5 min provided 28 mg (27%) of white solid after preparative HPLC purification. Reversed-phase HPLC analysis: 98% at 6.16 min. ¹H NMR (DMF-*d*₇): δ 0.69–0.92 (28H, m), 1.01–1.06 (3H, m), 1.17 (m), 1.42–1.53 (m), 1.53–1.68 (m), 1.70–2.28 (m), 2.28–2.46 (m), 2.74–2.88 (m), 2.89–3.00 (m), 3.04–3.06 (m), 3.15 (s), 3.18 (s), 3.24 (s), 3.40–3.47 (m), 3.48–3.58 (m), 3.59–3.68 (m), 3.71–3.76 (d), 3.96 (m), 4.14 (t), 4.23 (m), 4.38–4.52 (m), 4.58–4.76 (m), 4.89 (m), 5.95 (m), 7.01 (2H, s), 7.17–7.28 (5H, m), 7.77 (m), 7.89 (m), 7.96 (m), 8.04 (m), 8.17 (m), 8.28 (m), 8.38 (d), 8.47 (m). HRMS (ESI) calcd for C₆₀H₉₇N₁₀O₁₄ (MH)⁺ 1181.7186; found, *m/z* 1181.7164.

Maleimidocaproyl-PABC–MMAF (L3–MMAF). MeVal-Val-Dil-Dap-Phe-2-chlorotrityl resin (100 mg, 0.044 mmol) was treated with a solution of maleimidocaproyl-PAB-OCO-pNP (42 mg, 0.088 mmol, 2 equiv), 1-hydroxybenzotriazole (HOBt, 1 mg, 9 μmol, 0.1 equiv), and DIEA (30 μL, 0.176 mmol, 4 equiv) in DMF (3 mL) for 16 h. The resin was then filtered and washed with DMF (6 × 3 mL), CH₂Cl₂ (6 × 3 mL), and ethyl ether (6

× 3 mL). Cleavage from resin by treatment with 2% TFA in CH₂Cl₂ (4 mL) for 5 min followed by preparative HPLC purification provided 31 mg (66%) of white solid which was 99% pure by reversed-phase HPLC analysis (retention time 7.14 min). ¹H NMR (DMF-*d*₇): δ 0.76–0.98 (18H, m), 1.04 (2H, d), 1.12 (3H, m), 1.25–1.40 (m), 1.51–1.61 (m), 1.63–1.69 (m), 1.76–1.90 (m), 1.94–2.40 (m), 1.35–2.38 (m), 2.50–2.60 (m), 2.96 (s), 3.10 (s), 3.23 (s), 3.27 (s), 3.30 (s), 3.34 (s), 3.41–3.50 (m), 3.50–3.80 (m), 3.90–4.20 (m), 4.33–4.48 (m), 4.54–4.62 (m), 4.63–4.77 (m), 4.82–4.93 (m), 5.06–5.20 (m), 7.02 (2H, s), 7.36–7.21 (9H, m), 7.70 (2H, d), 8.11 (0.5H, d), 8.36 (0.5H, d), 10.00 (1H, br s). HRMS (ESI) calcd for C₅₇H₈₄N₇O₁₃ (MH)⁺ 1074.6127; found, *m/z* 1074.6095.

Maleimidocaproyl–MMAF (L4–MMAF). 6-Maleimidocaproic acid (37 mg, 0.176 mmol, 2 equiv) and HATU (67 mg, 0.176 mmol, 2 equiv) were dissolved in anhydrous DMF (3 mL), followed by the addition of DIEA (62 μL, 0.35 mmol, 4 equiv). The solution was then transferred to a 5 mL syringe containing MeVal-Val-Dil-Dap-Phe-2-chlorotrityl resin (200 mg, 0.088 mmol), and the mixture was agitated for 3 h. The resin was filtered, washed with DMF (6 × 3 mL), CH₂Cl₂ (6 × 3 mL), and ethyl ether (6 × 3 mL), and dried in vacuo. Drug–linker was cleaved off the resin by treatment with 2% TFA in CH₂Cl₂ (4 mL) for 5 min and then purified by preparative HPLC to give 57 mg (70%) of white solid. Reversed-phase HPLC analysis: 98% at 6.72 min. ¹H NMR (DMF-*d*₇): δ 0.78–0.96 (18H, m), 1.04 (2H, t), 1.12 (3H, m), 1.25–1.36 (m), 1.41 (2H, d), 1.46–1.65 (m), 1.73–1.87 (m), 1.88–2.07 (m), 2.08–2.26 (m), 2.32–2.48 (m), 2.48–2.67 (m), 2.79–2.84 (m), 2.96 (d), 3.02 (d), 3.10 (d), 3.23 (d), 3.27 (s), 3.30 (s), 3.34 (s), 3.45 (t), 3.52–3.61 (m), 3.62–3.80 (m), 3.93 (d), 4.09–4.28 (m), 4.54–4.78 (m), 4.82–4.91 (2H, m), 7.03 (2H, s), 7.21–7.35 (5H, m), 7.51 (0.5H, d), 8.11 (0.5H, d), 8.36 (0.5H, d), 8.48 (0.5H, d), 13.0 (br s). HRMS (ESI) calcd for C₄₉H₇₇N₆O₁₁ (MH)⁺ 925.5650; found, *m/z* 925.5636.

Maleimidocaproyl–[¹³C]MMAF (L4–[¹³C]MMAF) was prepared as described above starting from *N*-Fmoc-L-[ring-¹³C₆]-phenylalanine-2-chlorotrityl resin. LCMS (ESI): *m/z* 931.62 (MH)⁺.

Preparation of Antibody–Drug Conjugates. The conjugates with eight drug molecules per antibody were prepared as described previously (12, 19). Briefly, cBR96 or cAC10 (5–15 mg/mL) were mixed with DTT (10 mM, final) at 37 °C for 30 min, and the buffer was exchanged by elution through Sephadex G-25 resin with PBS containing 1 mmol/L diethylenetriaminepentaacetic acid. PBS containing 1 mmol/L diethylenetriaminepentaacetic acid was added to the reduced mAb bringing its final concentration to 2.5 mg/mL. The thiol concentration was ~8.4 thiols/mAb as measured by Ellman's reagent, DTNB. A 9.5-fold molar excess of linker–drug (L1–MMAF, L1–Dox (10), L1–MMAE (12), or L4–MMAE) was added to the reduced antibody at 4 °C for 1 h, and the conjugation reaction was quenched by adding a 20-fold excess of cysteine. The reaction mixture was concentrated by centrifugal ultrafiltration and buffer-exchanged through Sephadex G-25 equilibrated with PBS at 4 °C. The conjugate was then sterile filtered through a 0.2-μm filter.

cAC10 antibody–drug conjugates with four drugs per antibody were prepared by partial reduction of the mAb (14, 20) followed by reaction with desired linker–drug (L1–MMAF, L2–MMAF, L3–MMAF, or L4–MMAF). The antibody cAC10 (10 mg/mL) was partially reduced by addition of 3.0 molar equivalents of DTT at pH 8.0, followed by incubation at 37 °C for ~2 h. The reduction reaction was then chilled to ~10 °C and the excess DTT removed via diafiltration. The thiol concentration was determined by DTNB, and the SH/Ab ratio was found to be in the range of 3.8–4.5. The linker–drug was

then added to a linker–drug/thiol molar ratio of ~ 1.15 . The conjugation reaction was carried out in the presence of 15% v/v of DMSO. After conjugation, excess free cysteine (2 mol/L cysteine per mol/L linker–drug) was added to quench unreacted linker–drug to produce the cysteine–linker–drug adduct. The reaction mixture was purified and buffer-exchanged into PBS by diafiltration to obtain the partially loaded cAC10–linker–drug₄ conjugate. The molar ratio of drug substitution was determined according to previously published methods (14, 20).

Released Drug Identification. Lysosomal extracts of L540cy cells were prepared by swelling 2.4×10^8 cells in 9 mL of 0.25 M sucrose, 1 mM EDTA, and 10 mM HEPES (4-(2-hydroxyethyl)piperazine-1-ethansulfonic acid), pH 7.4. After 30 min on ice, cells were Dounce homogenized until >95% were broken as measured by Trypan Blue dye exclusion. Homogenates were centrifuged (3000g, 10 min, 4 °C) to pellet cellular debris, and the supernatant (4×10^7 cell equivalents per tube) was transferred to polyallomar ultracentrifuge tubes (13 × 51 mm) and centrifuged (17000g, 15 min, 4 °C) in a TLA100.3 rotor to isolate the lysosome-containing light mitochondrial pellet. Pellets were stored at -80 °C. The pellets were thawed and resuspended in 500 μ L of 50 mM sodium acetate pH 5.0 and 2 mM DTT. cAC10–L4–¹²C]MMAF₄, cAC10–L4–¹³C]MMAF₄, and cAC10–L4–^{12/13}C]MMAF₄ (50 μ g/mL) were independently added to one pellet. After three freeze/thaw cycles to break open lysosomes, samples were incubated for 24 h at 37 °C. Cold methanol (2 vol) was added to precipitate protein, the samples were centrifuged at 14000g to pellet debris, and 100 μ L of supernatant was analyzed by low resolution mass spectrometry as described above. Authentic cysteine–L4–MMAF was prepared by treating 100 μ M L4–MMAF with 1 mM cysteine in PBS at room temperature for 10 min.

In Vitro Growth Inhibition. Log phase cultures of cells were collected and cells plated at seeding densities ranging from 500 to 10000 cells/well according to predetermined conditions. After incubating 24 h to allow surface protein reconstitution, serial dilutions of test molecules were added and cultures incubated a further 4–6 days depending on cell line. Assessment of cellular growth and data reduction to generate IC₅₀ values was done using Alamar Blue (Biosource International, Camarillo, CA) dye reduction assay as previously described, according to previously published methods (12, 14, 15, 19). Briefly, a 40% solution (wt/vol) of Alamar Blue was freshly prepared in complete media just before cultures were added. Ninety-two hours after drug exposure, Alamar Blue solution was added to cells to constitute 10% culture volume. Cells were incubated for 4 h, and dye reduction was measured on a Fusion HT fluorescent plate reader (Packard Instruments, Meriden, CT).

In Vivo Therapy Experiments. For the localized, subcutaneous disease model of anaplastic large cell lymphoma, 5×10^6 Karpas 299 cells were implanted into the right flanks of C.B.-17 SCID mice. Therapy was initiated when the tumor size in each group of six animals averaged approximately 100 mm³. Treatments consisted of a single injection of solutions of the conjugates or controls in PBS intravenously (tail vein). Tumor volume was determined using the formula $(L \times W^2)/2$. For the disseminated ALCL model, 1×10^6 Karpas 299 were injected in the tail vein into C. B.-17 SCID mice. Single dose injection treatment was performed at 9 days after tumor injection. Mice that developed hind limb paralysis or other signs of significant disease were euthanized in accordance with Animal Care and Use Committee guidelines.

In Vivo Localization of Antibodies via Immunohistochemistry. When subcutaneous Karpas 299 tumor size reached 300 mm³, three animals per group received one injection of 10 mg antibody component/kg body weight of either cAC10–L1–MMAF₄ or cBR96–L1–MMAF₄ intravenously. Tumors were

Table 1. In Vitro Cytotoxicity of Auristatins

cell line	type	IC ₅₀ (nM) ^a		
		MMAE	MMAF	MMAF-OMe
Karpas 299	anaplastic large cell lymphoma	0.5	119	<0.001
H3396	breast carcinoma	0.1	105	<0.001
786-O	renal cell carcinoma	2.0	257	0.01
Caki-1	renal cell carcinoma	0.7	200	<0.001

^a Cells were exposed to the drugs, and the cytotoxic activities were determined 96 h later using Alamar Blue dye conversion as a measure of cell viability.

then removed and placed in optimal cutting temperature (OCT) compound (Sakura Finetec, Torrance, CA), and 5 μ m-thin frozen tissue sections were stained using immunohistochemistry evaluation. Briefly, frozen tissues on the slides were air-dried then fixed in 4% paraformaldehyde for 15 min at room temperature. Endogenous peroxidase activity was blocked using 0.6% H₂O₂ for 15 min. Additional blocking for endogenous biotin was done using the Avidin–Biotin Blocking kit (Vector Labs). Biotinylated-anti-human-Fc and biotinylated-anti-drug antibodies (both Seattle Genetics) were incubated on tissues at 2 μ g/mL concentration for 1 h at room temperature. Following incubation of slides with avidin conjugated to HRP (Vectastatin Elite ABC kit, Vector Labs), 3,3'-diabenzidine (DAB) was used as a substrate for HRP. Tissues were counterstained using hematoxylin, slides were dehydrated, and slips were applied. Images were taken using the Zeiss Axiovert light microscope.

TUNEL Assay. Apoptosis was evaluated by TUNEL Staining (In Situ Cell Death Detection Kit, TR Red, Roche Applied Science, Germany) according to the manufacturer's instructions. TUNEL staining was carried out on sections of frozen specimens embedded in OCT. Labeling was visualized by Zeiss Axiovert fluorescence microscopy.

RESULTS

Development of MMAF-Based Conjugates. The structure of the antimetabolic agent MMAE is shown in Figure 1. This drug has previously displayed IC₅₀ values in the range of 1–5 nM on hematologic cell lines (12, 15) and was designed for mAb-based targeted delivery using peptide-based linkers appended to the N-terminal methylvaline residue (12, 19). The synthesis of MMAE proceeded through a solution-phase route involving the coupling of the amino-protected N-terminal trimer to the C-terminal dimer. Due to the convergent nature of the process, it was possible for us to produce a large number of auristatins with varied solubilities, potencies, and pharmacokinetic properties. One molecule that emerged was MMAF-OMe (Figure 1), a C-terminal phenylalanine containing auristatin that remains one of the most potent drugs we have ever made (Table 1). We regarded MMAF-OMe as a prodrug of MMAF (Figure 1), with the potential of having facilitated intracellular uptake due to the presence of a neutral C-terminus. In addition, intracellular ester hydrolysis of MMAF-OMe should rapidly generate MMAF, a C-terminally charged molecule expected to have impaired membrane translocation capabilities. Therefore, MMAF was synthesized using solid-phase synthetic methodology and as expected was much less potent than MMAE on all cell lines tested (Table 1). In addition, the maximum tolerated dose in mice of MMAF (>16 mg/kg) was much higher than MMAE (1 mg/kg). Thus, MMAF was of great interest for targeted delivery, since the free drug had attenuated potency, lower toxicity, and much higher aqueous solubility compared to MMAE. Facilitated intracellular transport was expected to greatly enhance its activity.

Conjugates of MMAF were produced using the maleimido-caproyl-Val-Cit-PABC linker (L1, Figure 1) as described

Table 2. In Vitro Cytotoxicity of cAC10–MMAF ADCs and Free MMAF on a Panel of CD30⁺ and CD30⁻ Cell Lines

cell line tumor	type	IC ₅₀ (nM) ^a		
		cAC10–L1–MMAF ₄	cAC10–L4–MMAF ₄	MMAF
Karpas 299	anaplastic large cell lymphoma	0.057	0.059	119
SUP-M2	anaplastic large cell lymphoma	0.023	0.024	79.7
SU-DHL-1	anaplastic large cell lymphoma	0.007	0.045	34.7
SR-786	anaplastic large cell lymphoma	0.010	0.016	38.1
DEL	anaplastic large cell lymphoma	0.038	0.046	69.0
HH	cutaneous T-cell lymphoma	0.016	0.022	30.7
L540cy	Hodgkin's disease	0.060	0.085	70.4
HDLM-2	Hodgkin's disease	0.080	0.210	66.0
L428	Hodgkin's disease	0.021	0.058	68.0
KMH-2	Hodgkin's disease	0.009	0.068	45.4
RPMI 6666	Hodgkin's disease	0.091	0.180	164
WSU-NHL	Non-Hodgkin's lymphoma, CD30 ⁻	>25 ^b	>25 ^b	60.3
	mean (all lines)	0.034 ^c	0.066 ^d	70.4

^a Cytotoxicity was measured as indicated in Table 1. Concentrations of the ADCs are represented by the drug component. ^b Represents 1000 ng/mL mAb component. ^c Represents 1.36 ng/mL mAb component. ^d Represents 2.64 ng/mL mAb component.

earlier for MMAE (12, 19). The mAbs used were BR96 (17) and AC10 (19), chimeric IgG1 mAbs that bind to the LewisY antigen on human carcinomas, and the CD30 antigen on hematologic malignancies, respectively. Initial studies were undertaken with conjugates that had eight drugs/mAb, but more recent data demonstrating improved pharmacokinetic and toxicologic properties of conjugates having lower drug loadings (14) prompted us to investigate the activities of conjugates with fewer drugs/mAb. These were obtained through carefully controlled mAb disulfide reduction with limiting amounts of DTT sufficient to produce an average of four thiol groups/mAb. Alkylation with drugs bearing thiol-reactive maleimide functionalities led to the formation of conjugates having an average of four drugs/mAb. The resulting distributions of species were as previously described (20). It was found that the ability of the parent unmodified mAb to bind to cell-surface receptors was maintained in conjugates (12), and aggregate (<5%) and free drug levels (0.5%) were very low.

In Vitro Growth Inhibition. cAC10–L1–MMAF₄ was tested on a panel of both CD30 positive and negative cell lines as shown in Table 2. Cells were exposed to the ADCs continuously for 96 h, and the cytotoxic effects, as determined by Alamar Blue conversion, were compared to those of free MMAF. On a molar basis, the cAC10–L1–MMAF₄ was an average of >2200-fold more potent than free MMAF and was active on all the CD30-positive cell lines tested. The effects were immunologically specific, since WSU-NHL cells, which do not express detectable levels of the CD30 antigen, were unaffected by the conjugate. Limited studies were also undertaken with the cAC10–L1–MMAF-OMe₄-based conjugates, and it was found that they displayed IC₅₀ values on Karpas 299 (0.04 nM) and L540cy (0.11 nM) cells that were comparable to those of cAC10–L1–MMAF₄ (Table 2). This is consistent with the assumption stated earlier that the active form of MMAF-OMe is the free acid MMAF.

Further studies were undertaken with MMAF and the cBR96–L1–MMAF₈ conjugate on a LewisY positive human small cell lung carcinoma cell line (H69) and its P-glycoprotein-overexpressing counterpart H69/LX4 (18). The results were compared to doxorubicin and cBR96–L1–doxorubicin₈, a previously described conjugate with eight doxorubicin molecules/mAb (17, 21). H69/LX-4 cells were approximately 100-times less sensitive to doxorubicin compared to the parental cell (Figure 2A), while there was only a 3-fold difference with MMAF (Figure 2B). This trend extended to the conjugates, in that the drug resistant cell line was refractory to BR96–L1–doxorubicin₈ (Figure 2C), but quite sensitive to the corresponding MMAF conjugate (Figure 2D). These results have been confirmed on several MDR positive cell lines (data not shown),

in which it has been found that MMAF and MMAF-based immunoconjugates circumvent common forms of the MDR phenotype.

New Linker Technologies. The linker joining the drug to the mAb carrier plays a critical role in conjugate potency (3, 21–24). We applied our peptide linker technology to MMAF, based on its successful application with MMAE (12, 14, 15, 19, 20) and other drug classes (6, 9–11). To expand our understanding of the role that the linker plays in drug release and cytotoxicity, we made truncated linker–MMAF derivatives lacking the *p*-aminobenzyloxycarbonyl (PABC) self-immolative group (L2, Figure 1), the peptide (L3), and both the peptide and the PABC group (L4). The resulting modified drugs were attached to cAC10, forming ADCs with approximately four drugs/mAb. As expected from earlier work with related doxorubicin ADCs (6, 9–11), cAC10–L2–MMAF₄ was devoid of activity on Karpas 299 cells (Table 3). In contrast, both cAC10–L3–MMAF₄ and cAC10–L4–MMAF₄ were highly active, and were as active as the full-length construct (cAC10–L1–MMAF₄). Interestingly, ADCs with truncated linkers (L2, L3, and L4) were not substrates for human cathepsin B, which was a critical design element in forming the original proteolytically cleavable linker technology for doxorubicin (6, 9–11). The effects of the truncated linkers were drug-dependent, in that cAC10–L4–MMAE₈ had no cytotoxic activity above 50 nM (1000 ng/mL) on Karpas 299 cells.

The results prompted us to test cAC10–L4–MMAF₄ on the broad panel of hematologic cell lines shown in Table 2. The conjugate was active against all CD30 positive cell lines tested and had approximately half the activity of cAC10–L1–MMAF₄. In addition, the effects were immunologically specific, as CD30 negative SU-NHL cells were not affected by cAC10–L4–MMAF₄. Thus, MMAF can be attached to cAC10 through linkers not designed for proteolytic cleavage, without significant loss in potency.

The high potency and broad reactivity of cAC10–L4–MMAF₄ conjugates raised the question of precisely what drug related molecule might be released from the conjugate, since the L4 linker would appear to be noncleavable. To elucidate this, ¹³C-phenylalanine substituted L4–MMAF was synthesized and conjugated to cAC10. ¹²C, ¹³C, and a 1:1 mixture of ¹²C and ¹³C cAC10–L4–MMAF₄ were then incubated in lysosomal extracts of L540cy cells. Low molecular weight products were separated from proteins and were analyzed by LCMS. The identification of released drugs was based on the 6 mass unit shifts between the ¹²C and ¹³C derivatives of the drug. After inspection of mass spectra for such shifts, the only detectable drug-related molecule that was found was the cysteine adduct of maleimidocaproyl–MMAF (Figure 3). To confirm this, an

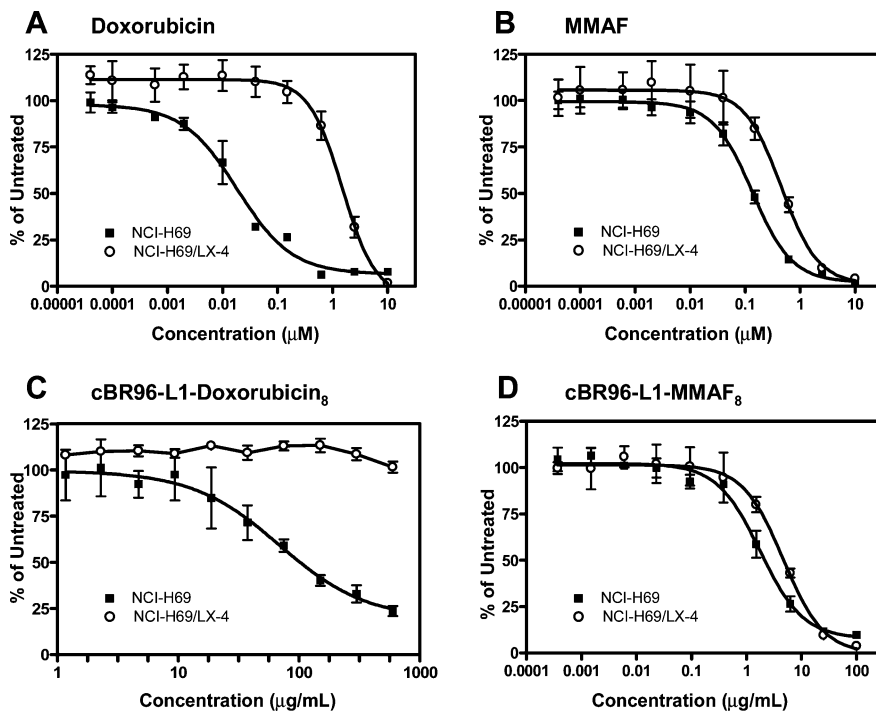


Figure 2. Cytotoxic effects of drugs (A, B) and cBR96-drug conjugates (C, D) on human small cell lung carcinoma cell line H69 (■) and its P-glycoprotein-overexpressing counterpart H69/LX-4 (○). Both cell lines are Lewis Y positive. The cells were incubated with either the drugs or the conjugates for 6 days, and the cytotoxic effects were determined by metabolism of Alamar Blue during the last 24 h of incubation.

Table 3. In Vitro Cytotoxicity of Drug–Linker Combinations

conjugate	target antigen	IC ₅₀ (nM) Karpas 299 cells ^a
cAC10–L1–MMAF ₄	CD30	0.03
cAC10–L2–MMAF ₄	CD30	>25
cAC10–L3–MMAF ₄	CD30	0.055
cAC10–L4–MMAF ₄	CD30	0.065
cAC10–L1–MMAE ₈	CD30	0.18
cAC10–L4–MMAE ₈	CD30	>50
cBR96–L1–MMAF ₄	Lewis Y	>25
cBR96–L4–MMAF ₄	Lewis Y	>25

^a Karpas 299 cells are CD30 positive, Lewis Y negative. Cytotoxicity was measured as indicated in Table 1. Concentrations of the ADCs are represented by the drug component. The numbers reported are representative of at least two independent experiments.

authentic sample of cysteine–L4–MMAF was synthesized and was shown to have the same elution and LCMS profile as the drug released from the cAC10–L4–MMAF₄ ADC (data not shown). The mAb is the likely source for cysteine in cysteine–L4–MMAF, since this was the residue to which the drug was attached. Thus, drug release takes place through mAb degradation. Studies are currently ongoing to identify other products that might also be formed and to establish the rates and extent of drug release.

Maximum Tolerated Doses. The maximum tolerated doses (MTDs) of the cAC10–MMAF conjugates were determined in BALB/c mice and in Sprague–Dawley rats and are defined as the highest dose that did not induce >20% weight loss, distress, or overt toxicities in any of the animals. This dose was generally within 20% of doses where such events took place. cAC10–L1–MMAF₄ has an MTD of 50 mg/kg in mice and 15 mg/kg in rats. The corresponding cAC10–L4–MMAF₄ ADC was much less toxic, having MTDs in mice and rats of >150 mg/kg (the highest dose tested, which resulted in no apparent toxicity) and 90 mg/kg in rats, respectively. This clearly indicates that the method by which the drug is attached to the mAb can have a pronounced effect on ADC tolerability, and the ADC lacking the peptide spacer within the linker was much less toxic than the peptide-based ADC.

Immunohistochemical Analyses. Studies were undertaken to determine if cAC10–L1–MMAF₄ localized into subcutaneous Karpas 299 tumors in nude mice. Animals were injected intravenously with cAC10–L1–MMAF₄ or cBR96–L1–MMAF₄ at 10 mg antibody component/kg body weight. Tumors were removed 24 h later, and frozen sections were evaluated for the presence of the mAb and drug components using immunohistochemistry with biotinylated anti-human-Fc and anti–MMAF mAbs as secondary antibodies, respectively. Figures 4A and 4C show that cAC10–L1–MMAF₄ accumulated much more efficiently within Karpas 299 tumors compared to the cBR96 nonbinding control ADC (Figure 4B and 4D). Since both the mAb (Figure 4A) and drug (Figure 4C) moieties were detected throughout the tumor, we conclude that the ADC is delivered as an intact molecule.

Additional studies were undertaken to determine the effects of ADC localization on apoptosis. Figure 4E demonstrates that there were significant levels of fragmented DNA in tumors of animals that received cAC10–L1–MMAF₄. This was established by TUNEL analysis, which measures bromodeoxyuridine incorporation into fragmented DNA. A nonbinding control ADC (Figure 4F) did not induce nearly this level of fragmentation, which is consistent with the localization data.

In Vivo Therapy Studies. The therapeutic effects of the ADCs were determined in nude mice with subcutaneous or disseminated Karpas 299 tumors. In animals with subcutaneous tumors, significant antitumor effects were obtained with a single injection of either cAC10–L1–MMAF₄ or cAC10–L4–MMAF₄, which were indistinguishably potent and active (Figure 5A). Nearly all animals that received single ADC injections at 2 mg antibody component/kg body weight were cured. In lowering the dose to 1 mg/kg, efficacy for both ADCs, dropped off in an apparently equal manner. At this dose, there were still two of six and three of six animals cured with the cAC10–L1–MMAF₄ and cAC10–L4–MMAF₄ ADCs, respectively.

To establish disseminated tumors, Karpas 299 cells were injected intravenously and allowed to distribute and become established before therapy was initiated 9 days later. In the

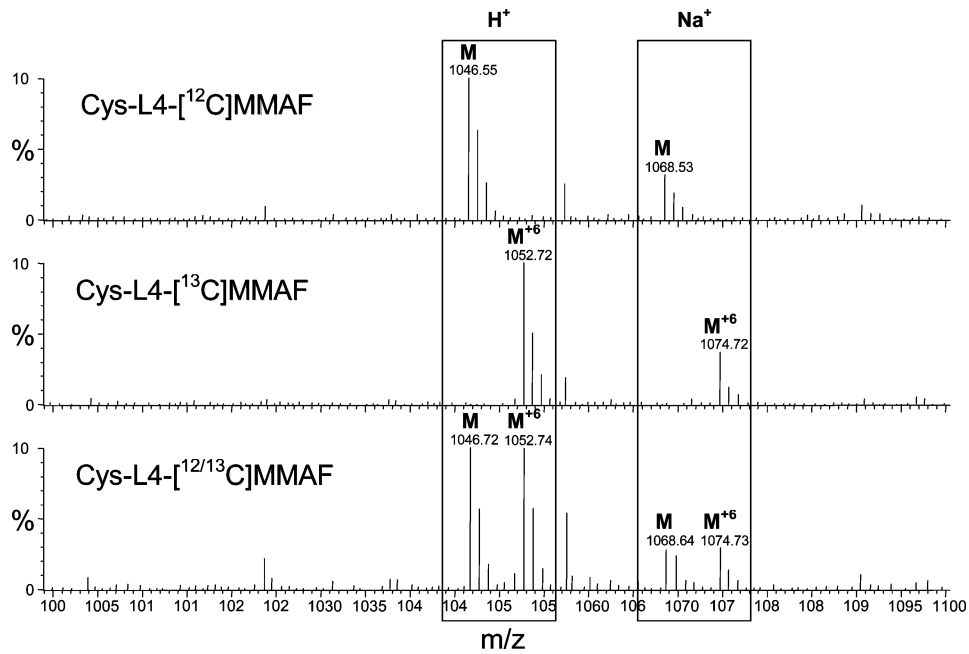


Figure 3. LCMS analysis of products released in lysosomal extracts of L540cy cells from cAC10-L4-MMAF₄ conjugate composed of [¹²C₆-Phe]-MMAF (top), [¹³C₆-Phe]-MMAF (middle), and a 1:1 mixture of these two conjugates (bottom). The fragments obtained from the co-mixture of the conjugates were analyzed for (M) and (M + 6) molecular ion clusters. Cysteine-L4-MMAF, *m/z* 1046/1052, was the only identifiable MMAF component.

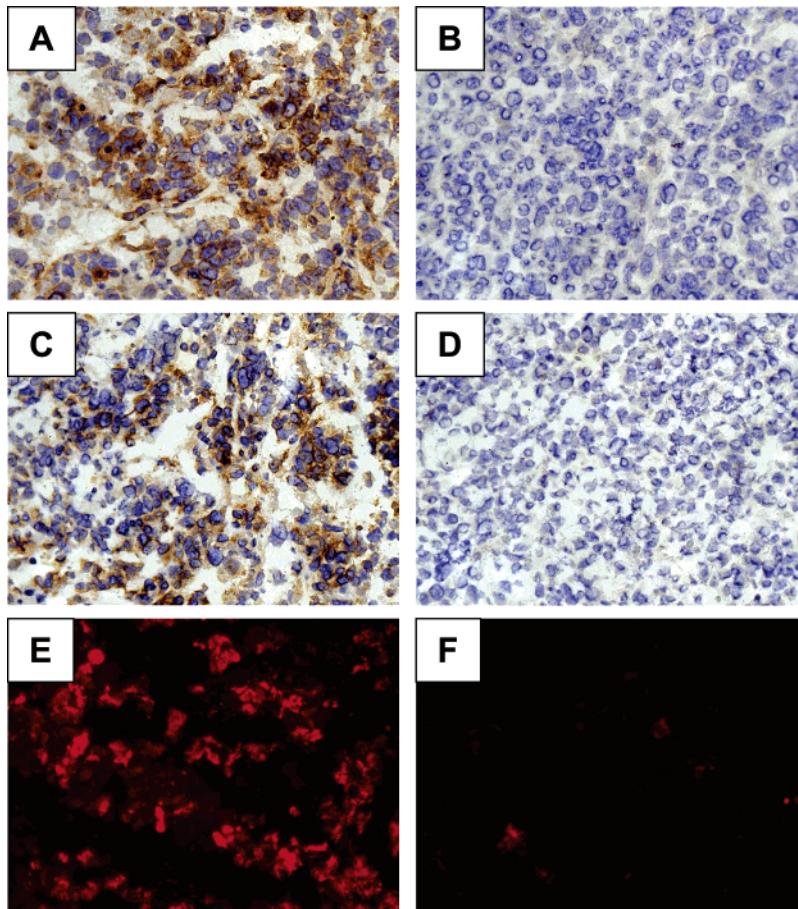


Figure 4. In vivo localization and activities of mAb-L1-MMAF₄ ADCs. Nude mice with subcutaneous Karpas 299 human tumors (cAC10 antigen positive, cBR96 antigen negative) were injected either with cAC10-L1-MMAF₄ (A, C, E) or with cBR96-L1-MMAF₄ (B, D, F) to investigate the localization and the induction of apoptosis on tumor xenografts. The presence of intratumoral mAb (A, B) and intratumoral MMAF (C, D) were determined by immunohistochemistry using either biotinylated anti-human-Fc or biotinylated anti-MMAF mAbs, respectively, as secondary antibodies. The tumors were excised and sectioned 24 h postconjugate administration. The apoptotic effect on Karpas 299 (E, F) were investigated using the TUNEL assay. The images were taken using 20× objectives on a Zeiss microscope.

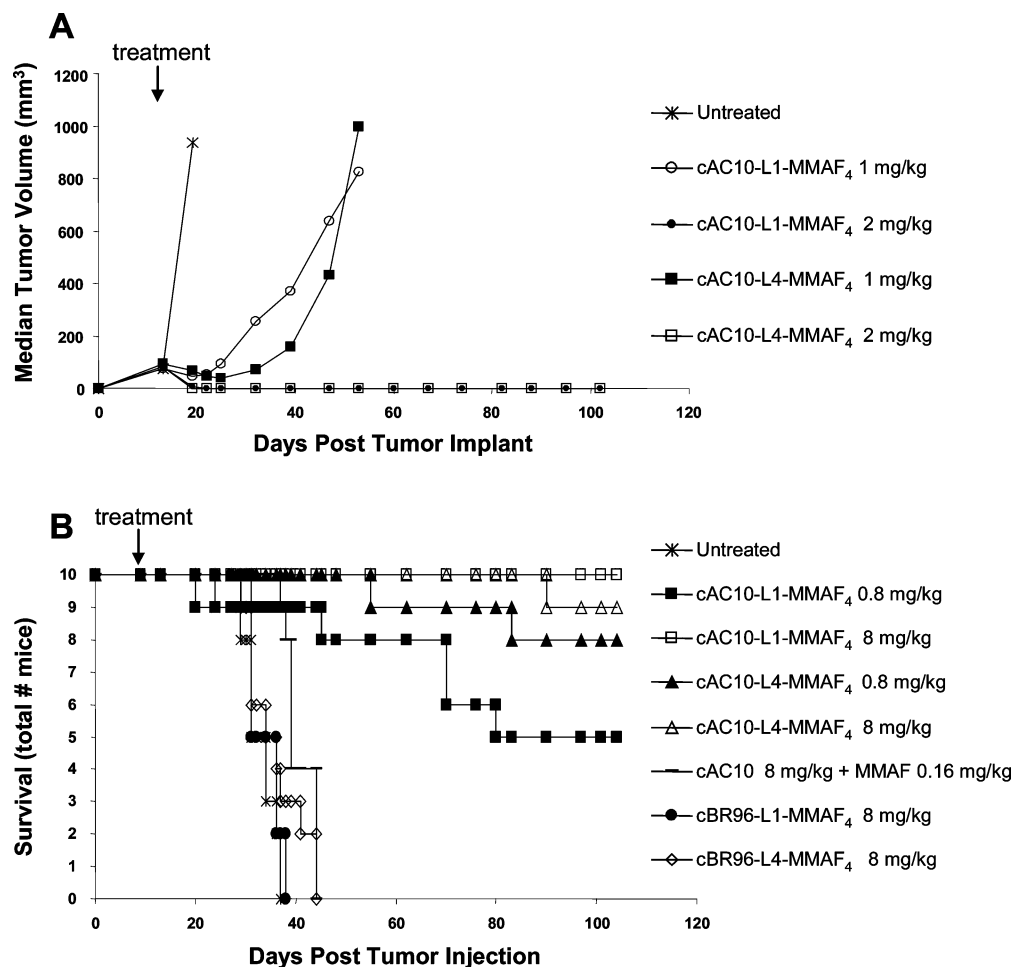


Figure 5. In vivo therapeutic efficacy of the conjugates in SCID mice. The data reported are representative of a number of independent studies. (A) Groups of mice (six/group) with subcutaneous Karpas 299 human ALCL tumors (cAC10 Ag⁺) of approximately 100 mm³ average in size were treated with cAC10-L1-MMAF₄ or cAC10-L4-MMAF₄ at 1 mg and 2 mg mAb component/kg. Cures: 1 mg/kg cAC10-L1-MMAF₄, two out of six; 1 mg/kg cAC10-L4-MMAF₄, three out of six; 2 mg/kg cAC10-L4-MMAF₄, five out of six; 2 mg/kg cAC10-L1-MMAF₄, six out of six. (B) Groups of mice (ten/group) with disseminated Karpas 299 ALCL tumor model (cAC10 Ag⁺, cBR96 Ag⁻) were treated on day 9 after tumor injection with cAC10-L1-MMAF₄, cAC10-L4-MMAF₄, cAC10 + unconjugated MMAF, cBR96-L1-MMAF₄, or cBR96-L4-MMAF₄ at the doses indicated.

absence of any treatment, all of the animals succumbed to disseminated disease by day 45. A single administration with either cAC10-L1-MMAF₄ or cAC10-L4-MMAF₄ was sufficient to cure most of the animals, with a slight dose response between 0.8 mg/kg and 8 mg/kg. The differences between the L1 and L4 linkers were not significant in this tumor model. One of the noteworthy findings in this experiment was the level of specificity. The nonbinding control ADCs, cBR96-L1-MMAF₄ and cBR96-L4-MMAF₄ were inactive, even at 8 mg/kg, which is 10-times the effective dose of the corresponding cAC10 ADCs. Thus, the MMAF conjugates exhibit pronounced activity at very well tolerated doses and are highly immunologically specific. Furthermore, the therapeutic window of cAC10-L4-MMAF₄ is measurably greater than that of cAC10-L1-MMAF₄, indicating that the linker technology plays a critical role in the design of effective ADCs that can be safely administered.

DISCUSSION

In this paper, we describe the synthesis and properties of MMAF, a new auristatin antimetabolic agent designed for attachment to mAbs through the secondary amino terminus. MMAF has much lower cytotoxic activity than MMAE (12, 14, 15, 19), presumably owing to the charged C-terminal phenylalanine group that impairs intracellular access. This hypothesis is

supported by the pronounced activity of MMAF-OMe, one of the most potent auristatins that we have developed. To further understand the precise cause of the attenuated activity of MMAF compared to the other drugs, studies are currently underway to measure intracellular concentrations in MDR positive and negative cell lines.

ADCs comprised of MMAF are distinct from those of other drugs, including MMAE. We show that the activities of MMAF are potentiated an average of 2200-fold when the drug is attached through the L1 linker to cAC10, a mAb that is efficiently taken up within the lysosomes of target cells (Table 2). With one exception that is likely cell line dependent (25), broad-scale drug potentiation through ADC formation is generally not seen, as evidenced by the in vitro results of MMAE (12) and other drug-containing ADCs (23, 24, 26, 27). The significance of this finding will become evident through detailed toxicological analyses, in which MMAE- and MMAF-based ADCs should be quite distinct if systemically released drug contributes to ADC toxicity.

One of the most striking results from this work surrounds the unexpected activity of cAC10-L4-MMAF₄, an ADC that has no built-in provision for drug release. Purified human enzymes that we have tested were unable to facilitate release of MMAF or any identifiable MMAF fragments, yet cAC10-L4-MMAF₄ is highly potent, both in vitro and in vivo. We

propose that the mechanism of drug release involves complete degradation of the mAb, based on the identification of the cysteine adduct of L4-MMAF. The finding that the released drug from the L4 linker is highly modified might explain why such truncated linker technology is not uniformly applicable, since many drugs lose activity as a result of derivatization. Indeed, MMAE was not tolerant of such modification (Table 3), and corresponding doxorubicin ADCs have also proven to be inactive (data not shown). The data in Table 3 also demonstrate that the various linkers within the MMAF ADC family provide a range of cytotoxic activities. The fact that cAC10-L2-MMAF₄ was inactive suggests that the released agent from the L2-MMAF ADC is highly attenuated in activity. We focused on cAC10-L4-MMAF₄ for further work rather than cAC10-L3-MMAF₄, since the PABC group in the L3 linker is hydrophobic and apparently unnecessary for activity.

The objective of the investigations with various linkers was to determine if the mode of drug release could affect ADC therapeutic index. We found that cAC10-L4-MMAF₄ differed from cAC10-L1-MMAF₄ by an average of only 2-fold on a large panel of hematologic cell lines (Table 2) although L1 linker cleavage is quite facile through enzymes such as cathepsin B, while drug release through the L4 linker requires antibody degradation. This provided the basis for in vivo experiments, since we anticipated that the different pathways required for drug elimination could strongly influence the therapeutic windows of the ADCs. Indeed, it was found that cAC10-L4-MMAF₄ was tolerated at significantly higher doses in rodents than cAC10-L1-MMAF₄ but was equally efficacious in vivo. Our results suggest that the therapeutic window is increased by at least 3-fold through the L4 linker system.

We are in the process of assessing several aspects of MMAF linker technology. Current studies include the application of mAb-L4-MMAF ADCs directed against antigens on an array of tumor types. Our preliminary data suggest that such ADCs are broadly active against hematologic malignancies but are only sporadically effective in the carcinomas we have evaluated. We are gaining insight into the factors that influence activity by assessing bound and unbound drug both inside and outside target cells. In addition, we are characterizing the mechanisms of drug release in target and nontarget cells in order to further understand the principles that influence activity and toxicity.

Supporting Information Available: Synthetic schemes for all linker-drugs. This material is available free of charge via the Internet at <http://pubs.acs.org/BC>.

LITERATURE CITED

- Adams, G. P., and Weiner, L. M. (2005) Monoclonal antibody therapy of cancer. *Nat. Biotechnol.* **23**, 1147–57.
- Baker, M. (2005) Upping the ante on antibodies. *Nat. Biotechnol.* **23**, 1065–72.
- Wu, A. M., and Senter, P. D. (2005) Arming antibodies: prospects and challenges for immunoconjugates. *Nat. Biotechnol.* **23**, 1137–46.
- Lambert, J. M. (2005) Drug-conjugated monoclonal antibodies for the treatment of cancer. *Curr. Opin. Pharmacol.* **5**, 543–9.
- Payne, G. (2003) Progress in immunoconjugate cancer therapeutics. *Cancer Cell* **3**, 207–12.
- Dubowchik, G. M., and Walker, M. A. (1999) Receptor-mediated and enzyme-dependent targeting of cytotoxic anticancer drugs. *Pharmacol. Ther.* **83**, 67–123.
- Smith, S. V. (2004) Technology evaluation: cantuzumab mersansine, ImmunoGen. *Curr. Opin. Mol. Ther.* **6**, 666–74.
- DiJoseph, J. F., Popplewell, A., Tickle, S., Ladyman, H., Lawson, A., Kunz, A., Khandke, K., Armellino, D. C., Boghaert, E. R., Hamann, P., Zinkewich-Peotti, K., Stephens, S., Weir, N., and Damle, N. K. (2005) Antibody-targeted chemotherapy of B-cell lymphoma using calicheamicin conjugated to murine or humanized antibody against CD22. *Cancer Immunol. Immunother.* **54**, 11–24.
- Dubowchik, G. M., and Firestone, R. A. (1998) Cathepsin B-sensitive dipeptide prodrugs. 1. A model study of structural requirements for efficient release of doxorubicin. *Bioorg. Med. Chem. Lett.* **8**, 3341–6.
- Dubowchik, G. M., Firestone, R. A., Padilla, L., Willner, D., Hofstead, S. J., Mosure, K., Knipe, J. O., Lasch, S. J., and Trail, P. A. (2002) Cathepsin B-labile dipeptide linkers for lysosomal release of doxorubicin from internalizing immunoconjugates: model studies of enzymatic drug release and antigen-specific in vitro anticancer activity. *Bioconjugate Chem.* **13**, 855–69.
- Dubowchik, G. M., Mosure, K., Knipe, J. O., and Firestone, R. A. (1998) Cathepsin B-sensitive dipeptide prodrugs. 2. Models of anticancer drugs paclitaxel (Taxol), mitomycin C and doxorubicin. *Bioorg. Med. Chem. Lett.* **8**, 3347–52.
- Doronina, S. O., Toki, B. E., Torgov, M. Y., Mendelsohn, B. A., Cervený, C. G., Chace, D. F., DeBlanc, R. L., Gearing, R. P., Bovee, T. D., Siegall, C. B., Francisco, J. A., Wahl, A. F., Meyer, D. L., and Senter, P. D. (2003) Development of potent monoclonal antibody auristatin conjugates for cancer therapy. *Nat. Biotechnol.* **21**, 778–84.
- Sanderson, R. J., Hering, M. A., James, S. F., Sun, M. M., Doronina, S. O., Siadak, A. W., Senter, P. D., and Wahl, A. F. (2005) In vivo drug-linker stability of an anti-CD30 dipeptide-linked auristatin immunoconjugate. *Clin. Cancer Res.* **11**, 843–52.
- Hamblett, K. J., Senter, P. D., Chace, D. F., Sun, M. M., Lenox, J., Cervený, C. G., Kissler, K. M., Bernhardt, S. X., Kopcha, A. K., Zabinski, R. F., Meyer, D. L., and Francisco, J. A. (2004) Effects of drug loading on the antitumor activity of a monoclonal antibody drug conjugate. *Clin. Cancer Res.* **10**, 7063–70.
- Law, C. L., Cervený, C. G., Gordon, K. A., Klussman, K., Mixan, B. J., Chace, D. F., Meyer, D. L., Doronina, S. O., Siegall, C. B., Francisco, J. A., Senter, P. D., and Wahl, A. F. (2004) Efficient elimination of B-lineage lymphomas by anti-CD20-auristatin conjugates. *Clin. Cancer Res.* **10**, 7842–51.
- Wahl, A. F., Klussman, K., Thompson, J. D., Chen, J. H., Francisco, L. V., Risdon, G., Chace, D. F., Siegall, C. B., and Francisco, J. A. (2002) The anti-CD30 monoclonal antibody SGN-30 promotes growth arrest and DNA fragmentation in vitro and affects antitumor activity in models of Hodgkin's disease. *Cancer Res.* **62**, 3736–42.
- Trail, P. A., Willner, D., Lasch, S. J., Henderson, A. J., Hofstead, S., Casazza, A. M., Firestone, R. A., Hellstrom, I., and Hellstrom, K. E. (1993) Cure of xenografted human carcinomas by BR96-doxorubicin immunoconjugates. *Science* **261**, 212–5.
- Reeve, J. G., Rabbitts, P. H., and Twentyman, P. R. (1989) Amplification and expression of *mdr1* gene in a multidrug resistant variant of small cell lung cancer cell line NCI-H69. *Br. J. Cancer* **60**, 339–42.
- Francisco, J. A., Cervený, C. G., Meyer, D. L., Mixan, B. J., Klussman, K., Chace, D. F., Rejniak, S. X., Gordon, K. A., DeBlanc, R., Toki, B. E., Law, C. L., Doronina, S. O., Siegall, C. B., Senter, P. D., and Wahl, A. F. (2003) cAC10-vcMMAE, an anti-CD30-monomethyl auristatin E conjugate with potent and selective antitumor activity. *Blood* **102**, 1458–65.
- Sun, M. M., Beam, K. S., Cervený, C. G., Hamblett, K. J., Blackmore, R. S., Torgov, M. Y., Handley, F. G., Ihle, N. C., Senter, P. D., and Alley, S. C. (2005) Reduction-alkylation strategies for the modification of specific monoclonal antibody disulfides. *Bioconjugate Chem.* **16**, 1282–90.
- Trail, P. A., Willner, D., Knipe, J., Henderson, A. J., Lasch, S. J., Zoekler, M. E., TrailSmith, M. D., Doyle, T. W., King, H. D., Casazza, A. M., Braslawsky, G. R., Brown, J., Hofstead, S. J., Greenfield, R. S., Firestone, R. A., Mosure, K., Kadow, K. F., Yang, M. B., Hellstrom, K. E., and Hellstrom, I. (1997) Effect of linker variation on the stability, potency, and efficacy of carcinoma-reactive BR64-doxorubicin immunoconjugates. *Cancer Res.* **57**, 100–5.
- Chari, R. V., Martell, B. A., Gross, J. L., Cook, S. B., Shah, S. A., Blattler, W. A., McKenzie, S. J., and Goldmacher, V. S. (1992) Immunoconjugates containing novel maytansinoids: promising anticancer drugs. *Cancer Res.* **52**, 127–31.

- (23) Hamann, P. R., Hinman, L. M., Beyer, C. F., Greenberger, L. M., Lin, C., Lindh, D., Menendez, A. T., Wallace, R., Durr, F. E., and Upešlacis, J. (2005) An anti-MUC1 antibody-calicheamicin conjugate for treatment of solid tumors. Choice of linker and overcoming drug resistance. *Bioconjugate Chem.* *16*, 346–53.
- (24) Hamann, P. R., Hinman, L. M., Beyer, C. F., Lindh, D., Upešlacis, J., Shochat, D., and Mountain, A. (2005) A calicheamicin conjugate with a fully humanized anti-MUC1 antibody shows potent antitumor effects in breast and ovarian tumor xenografts. *Bioconjugate Chem.* *16*, 354–60.
- (25) Hamann, P. R., Hinman, L. M., Hollander, I., Beyer, C. F., Lindh, D., Holcomb, R., Hallett, W., Tsou, H. R., Upešlacis, J., Shochat, D., Mountain, A., Flowers, D. A., and Bernstein, I. (2002) Gemtuzumab ozogamicin, a potent and selective anti-CD33 antibody-calicheamicin conjugate for treatment of acute myeloid leukemia. *Bioconjugate Chem.* *13*, 47–58.
- (26) Miller, M. L., Roller, E. E., Wu, X., Leece, B. A., Goldmacher, V. S., Chari, R. V., and Ojima, I. (2004) Synthesis of potent taxoids for tumor-specific delivery using monoclonal antibodies. *Bioorg. Med. Chem. Lett.* *14*, 4079–82.
- (27) Ojima, I., Geng, X., Wu, X., Qu, C., Borella, C. P., Xie, H., Wilhelm, S. D., Leece, B. A., Bartle, L. M., Goldmacher, V. S., and Chari, R. V. (2002) Tumor-specific novel taxoid-monoclonal antibody conjugates. *J. Med. Chem.* *45*, 5620–3.

BC0502917